

# Metallurgical and acoustical comparisons for a brass pan with a Caribbean steel pan standard

L. E. MURR, E. V. ESQUIVEL, A. A. BUJANDA, N. E. MARTINEZ, K. F. SOTO,  
A. S. TAPIA, S. LAIR, A. C. SOMASEKHARAN

*Department of Metallurgical and Materials Engineering, The University of Texas at El Paso,  
El Paso, TX 79968, USA*

*E-mail: fekberg@utep.edu*

C. A. C. IMBERT

*Department of Mechanical Engineering, The University of the West Indies, St. Augustine,  
Trinidad and Tobago*

R. KERNS, S. IRVINE, S. LAWRIE

*Panyard, Inc., 1216 California Ave., Akron, OH 44314, USA*

The development and fabrication of  $\alpha$ -brass pans, including the sinking of the pan head in the traditional manner using a hammer and patterning musical notes and their turning is compared with a low-carbon steel (Caribbean-type) pan as a standard. In this study these experimental pans are fabricated by welding the  $\alpha$ -brass or low-carbon steel platforms to a low-carbon steel hoop and side metal or skirt. These pans are 2.54 cm larger in diameter than pans traditionally fabricated from 55-gallon barrels. The corresponding pan head materials are examined by optical and electron microscopy and hardness profiles are measured as well. Deformation is shown to influence the acoustic response of ideal, flat, circular discs of both the  $\alpha$ -brass and low-carbon steel as well as 316L stainless steel. The frequency-amplitude-time spectra for common octave ranges are compared and chromatic tones are shown for the  $\alpha$ -brass as well as the low-carbon steel standard. These results indicate that a wide range of hard metals or alloys can be used to produce musical pan instruments. © 2004 Kluwer Academic Publishers

## 1. Introduction

The development and evolution of the Caribbean steel drum (or steelpan) since its inception in its present form around 1946 in Trinidad and Tobago has been constrained to the musical platform afforded by the doming and patterning of notes on commercial 55-gallon barrel heads. Pans containing from 3 to 32 notes representing virtually 9 orchestral voices have been patterned and tuned on this platform with tonal ranges from roughly 55 to 1400 Hz (from  $A_1$  to  $F_6$ ), corresponding to the musical range of a baby grand piano.

A subcategory of musical percussion instruments is the *Membranophone*, which produces sound through the vibration of a stretched membrane or skin. The most important type of membranophone is the drum. The steelpan falls under a different subcategory, that of *Idiophones* and as a sub-class—Vibration of Shells. The steelpan or pan is clearly not a drum. References to the pan as a drum in scientific literature, is unfortunate and incorrect (despite its construction from steel drums). The “drum” terminology and its implications can cause serious misunderstanding especially where the interpretations and applications of the results of this study are concerned. Consequently, we will consistently refer to the steelpan or pan throughout.

For more than a half-century, note patterns and pan voices have evolved by intuition and trial and error as a unique art form. The steelpan, by its nature, is a complex, non-linear, multi-harmonic, chromatic-tone instrument. The fact that the notes exist on the same low-carbon steel (dome) head or acoustic platform means that sympathetic resonances occur between note zones, which are tuned to a fundamental or tonic ( $f$ ), one octave ( $2f$ ) and additional overtones close to octaves ( $nf$ , where  $n = 3, 4, 5 \dots$ ). This produces the uniquely characteristic sound of the Caribbean steel pan.

Because the notes and note patterns to produce specific orchestral voices or tonal ranges are accommodated on a standard platform, optimization is not always possible. In addition, the method of creating the domed platform using sledge hammers or mechanized hammers can produce varying note thicknesses from the lower octaves near the rim or top of the pan to higher octaves at the bottom of the dome where the note sizes are smaller in the higher range instruments.

Correspondingly, the deformation of the low-carbon steel varies from roughly 10% near the pan rim (or top) to nearly 50% at the bottom of the instrument with the highest range (soprano, or tenor pan as it is traditionally called) [1]. It should be noted that it is not necessary for

the note thickness to be constant across the note. The general dynamics are the same. Tuning also requires the patterned pan head to be heated or “burned”, and this process, although originally accomplished to burn away residual oil or paint, has more recently been characterized as metallurgical aging of the low-carbon steel, where the carbon content also plays a role in optimizing the ageing treatment [1–5].

The 55-gallon, low-carbon steel barrel, with a diameter of 57.2 cm and cylindrical side and flat ends of 20 (0.8 mm) and 18 (1.15 mm) gauge sheet respectively, has become the standard for producing the musical instruments which are commonly referred to as the Caribbean steelpan (or steel drum).

However, there is no reason why the platform dimensions cannot be altered or the material changed. It is in fact relatively unknown how common metals such as brass, stainless steel or aluminum would perform as a musical platform, or how the fabrication routine would have to be altered to accommodate a metal or alloy other than low-carbon steel.

In this research program low-carbon steel and 70/30 ( $\alpha$ ) brass pan heads were attached to low-carbon steel skirts by means of a low-carbon steel hoop welded to the head and skirt. The pan heads were 59.7 cm in diameter in contrast to standard 57.2 cm diameter, 55-gallon containers. The pan heads were hammered into a standard concave dome. Comparisons were made of the corresponding sheet metal microstructures utilizing optical and transmission electron microscopy and microhardness along with acoustic spectrum comparisons for tuned notes and note sequences.

## 2. Note modeling and analytical considerations

Considering steel pan notes to be represented by ellipsoidal shells characterizing a complex dynamical system of interacting, non-linear vibrational modes on a single note; with energy exchanges between these modes, Achong [6, 7] has developed the following set of non-linear equations:

$$\begin{aligned}
 F_d(t) = & F_o + \ddot{u}_{nd} + \omega_{nd}^2 u_{nd} + \mu_{nd} \dot{u}_{nd} \\
 & + \sum_{j=1}^{\infty} \sum_{\kappa=1}^{\infty} \alpha_{j\kappa n}^{(d)} u_{jd} u_{\kappa d} \\
 & + \sum_{i=1}^{\infty} \sum_{j=1}^{\infty} \sum_{k=1}^{\infty} \gamma_{ip,jp,kp}^{(nd)} u_{ip} u_{jp} u_{kp} \\
 & + \sum_{j=1}^{\infty} \sum_{k=1}^{\infty} \sum_{p=1}^2 \beta_{jp,kp}^{(nd)} U_{jp} U_{kp} \\
 & + \sum_{j=1}^{\infty} \Gamma_{jd}^{(nd)} u_{jd}
 \end{aligned} \tag{1}$$

where the eight force components are defined as follows with respect to the driving force imparted by the impact of the mallet with the note surface,  $F_d(t)$ :

- (1)  $F_o$  is a static force directed upward against the mallet force and arising from in-plane stresses;
- (2)  $\ddot{u}_{nd}$  is the note surface acceleration for the  $n$ th mode;
- (3)  $\omega_{nd}^2 u_{nd}$  is a restoring force driving the  $n$ th mode at a frequency  $\omega_{nd}$ ;
- (4)  $\mu_{nd} \dot{u}_{nd}$  is a material damping force for the  $n$ th mode;
- (5) represents quadratic forces arising from the dome geometry that drive vibrational motions at frequencies  $\omega_{jd} \pm \omega_{kd}$ ;
- (6) is characteristic of cubic forces which arise from the stretching of the vibrating note and drive vibrations at all combinations of frequencies formed by  $\omega_{id}$ ,  $\omega_{jd}$ ,  $\omega_{kd}$ ;
- (7) represents quadratic coupling forces between two domains on the drum surface such as sympathetic pairs; and
- (8) is a linear coupling of forces between two domains on the pan surface such as note-note and note-skirt.

In Equation 1,  $d$  defines the source domain and  $\bar{d}$  the receiver domain;  $u_{nd}$  and  $\omega_{nd}$  refer to the surface displacements and natural frequencies and  $\mu_{nd}$  are the damping coefficients. The  $\alpha$  and  $\beta$  terms in Equation 1 refer to quadratic coupling between domains, while the  $\gamma$  terms are the cubic coupling coefficients between modes on a note domain and  $\Gamma_{jd}^{(nd)}$  is the linear coupling coefficient between domains [6]. Equation 1 describes all the musical and other dynamical features of the steelpan but it places no elastic or materials restrictions on the metal, and therefore it applies to steel, brass, or any other metal. It is presented here to simply serve as a symbolic/graphic representation of the instrument's complexity.

A similar, non-linear equation has been developed by Achong [8] to describe the dimensionless eigen frequencies with reference to Fig. 1:

$$\begin{aligned}
 \omega_n^2 = & \frac{1}{12} \bar{L}_n(\psi_n) + 8(1 + \nu) \left( \frac{H_0}{h} \right)^2 \{ \bar{M}_n(Q^2 \psi_n) \\
 & - \frac{1}{2} (1 + \nu) \bar{P}_n(Q \psi'_n, Q) \} \\
 & - (\check{N}_C + \check{N}_T) \bar{X}_n(\psi_n) + 2(1 + \nu) \left( \frac{H_0}{h} \right) \\
 & \times \{ \bar{Y}_n(\psi'_0, Q \psi'_n) + \bar{Y}_n(\psi'_n, Q \psi'_0) \\
 & + \bar{M}_n(Q \psi'_0 \psi'_n) - \bar{S}_n(\psi'_0, \psi'_n, Q) \\
 & - \bar{V}_n(Q \psi_0 \psi'_n) - \bar{V}_n(Q \psi_n \psi'_0) \} \\
 & - \frac{3}{2} \bar{V}'_n(\psi'_n \psi'^2) + \frac{1}{2} \bar{Z}_n(\psi'_n \psi'^2) \\
 & + \bar{Z}_n(\psi'_0, \psi'_0 \psi'^n)
 \end{aligned} \tag{2}$$

where  $\bar{L}_n$ ,  $\bar{M}_n$ ,  $\bar{P}_n$ , etc., imply so-called functionals,  $G$  (variable<sub>1</sub>, variable<sub>2</sub>, ...) defined by the generic

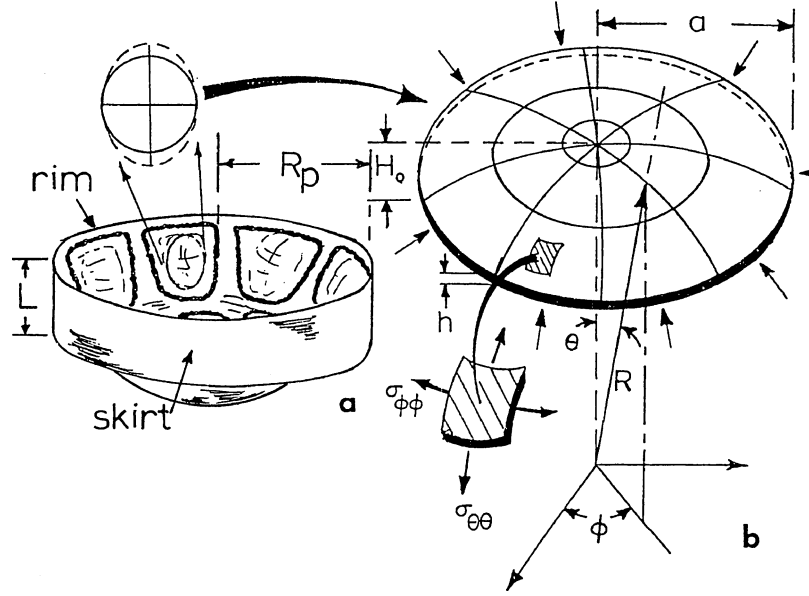


Figure 1 Schematic representations of the conventional Caribbean steopan. (a) Drum with patterned note zones in which elliptical notes (represented by a hemispherical shell) are fashioned. The important pan dimensions are noted. (b) Circular shell showing geometrical parameters.  $\sigma_{\phi\phi}$  and  $\sigma_{\theta\theta}$  represent the stress components of the shell element. (After Ref. [5]).

functional,  $G$  (Equation 3):

$$\bar{G}_n(\text{var}_1, \dots) = \frac{\int_0^1 G(\text{var}_1, \dots) \psi_n x dx}{\int_0^1 \psi_n^2 x dx} \quad (3)$$

and  $\psi_0$  and  $\psi_n$  imply static displacements and modal coordinates respectively,  $\nu$  is Poisson's ratio,  $H_0/h$  is the rise factor illustrated in Fig. 1b for a shell of circular planform, and  $Q$  describes the departure from true sphericity or the shell surface imperfections or irregularities ( $Q = 1$  for perfectly hemispherical, circular shells). The term  $(\check{N}_C + \check{N}_T)$  as a factor denotes compressive and thermal stress dependence, respectively [8] (Equation 2):

$$\check{N}_C = \frac{N_C a^2 (1 - \nu^2)}{E h^3} \quad (4)$$

and

$$\check{N}_T = \alpha \delta T (1 + \nu) \left( \frac{a}{h} \right)^2 \quad (5)$$

where  $N_C$  is a uniform compression (arrows around the note in Fig. 1),  $a$  is the ideal planform (note) radius,  $h$  is the note thickness as shown in Fig. 1,  $E$  is the elastic (Young's) modulus,  $\alpha$  the thermal expansion coefficient, and  $\delta T$  is the uniform temperature variation in the note. Like Equation 1, Equation 2 is also intended to serve as a symbolic/graphic representation for the frequency domain, and since  $\omega_n$  is dimensionless, the small amplitude modal frequencies for each note,  $f_n$  (in Hertz), can be expressed ideally as:

$$f_n = \frac{\omega_n}{2\pi} \sqrt{\frac{E}{\rho(1 - \nu^2)}} \left( \frac{h}{a^2} \right) \quad (6)$$

where  $\rho$  is the density of the note metal. It can be noted in Equations 2 and 6 that three geometric or dimensional parameters influence the note frequencies: the note thickness,  $h$ , the ideal note radius  $a$ , and the rise

of the note,  $H_0$  (or the rise factor,  $H_0/h$ ). For large low-frequency and mid-range notes the thickness across the note can vary from roughly 5 to 10 per cent.

The pan skirt provides an acoustical baffle to reduce sound interference from the top and bottom head surfaces. It also vibrates sympathetically and radiates sound. For a cylindrical skirt of length  $L$ , radius  $R_p$ , thickness,  $h$  (Fig. 1a) its natural frequencies are given by the Soedel formulation [9]:

$$f_{mn} = \frac{1}{2\pi} \sqrt{\frac{E}{\rho}} \times \left[ \frac{\eta_m^4}{R_p^2 L^4 \left( \frac{n^2}{R_p^2} + \frac{R_m^2}{L^2} \right)} + \frac{h^2}{12(1 - \nu^2)} \left( \frac{n^2}{R_p^2} + \frac{\eta_m^2}{L^2} \right)^2 \right]^{1/2} \quad (7)$$

where  $\eta_m$  are the roots of the analogous clamped-free beam problem with  $m$  (1, 2, 3...) representing the axial mode numbers. The index,  $n$  (0, 1, 2, 3...) represents the circumferential wave numbers identifying the swaying ( $n = 1$ ), ovalling ( $n = 2$ ), and breathing ( $n > 2$ ) modes [9, 10].

The coupling between the note areas and the skirt has been shown to be fairly weak; the vibration amplitude is more than 200 times less than in a note area for a standard carbon-steel pan [11]. In spite of the fact that the sound radiation from the skirt does not contribute significantly to the overall sound level, the vibrational spectrum of the skirt is sufficiently different from that of the note area to have some influence on the pan timbre.

Changing the pan platform (or note planform) from the traditional low-carbon steel to  $\alpha$ -brass (cartridge brass: 70Cu-30Zn) will alter the eigen frequencies and the small amplitude modal frequencies for the notes because Poisson's ratio, the density, and the elastic constant will change as illustrated in Table I. The values of  $[E/\rho(1 - \nu^2)]^{1/2}$  represent the longitudinal sound

TABLE I Comparison of low-carbon steel and brass pan properties (starting materials)

Pan head material	Young's modulus ( $E$ ) GPa	Density ( $\rho$ ) Mg/m <sup>3</sup>	Poisson's ratio ( $\nu$ )	Sound velocity (m/s)	$n$ (Equation 8)	$K$ (GPa) (Equation 8)	Crystal structure & lattice parameter	Grain size ( $\mu\text{m}$ )	Vickers hardness (VHN)
Low-carbon (0.06%) steel	200	7.9	0.28	5900	0.26	0.53	BCC $a = 2.87\text{\AA}$	20	118
$\alpha$ -brass (70/30)	110	8.5	0.32	4700	0.50	0.90	FCC $a = 3.68\text{\AA}$	30	116

velocity which is reduced by as much as 21% in the brass pan (4700 m/s) from the low-carbon-steel pan (5900 m/s). Correspondingly, in order to maintain the same note tonic in an  $\alpha$ -brass pan in contrast to a standard low-carbon steel pan, the ideal (circular) note sizes (radii) must be reduced by roughly 15% (Equation 6 and including some rise,  $H_0$  in Equation 1) while maintaining the same note thickness (or thickness variation).

In the sinking of the dome by hammering as noted previously, the thickness varies non-linearly, decreasing by roughly 10% near the rim where the low (frequency) notes are placed, and by 40 to 50% at the bottom of the sunken pan head of the lead instrument [1]. The forming of the dome will be governed to some extent by the corresponding dome metal stress-strain diagram, which for polycrystalline materials is approximated by the Ludwik-Holloman equation:

$$\sigma = K \varepsilon^n \quad (8)$$

where  $\sigma$  is the stress,  $K$  is a constant,  $\varepsilon$  is the total strain, and  $n$  is the work-hardening or strain-hardening coefficient. It can be noted from Table I that the value of  $n$  is essentially doubled for the brass in contrast to low-carbon steel. Consequently, brass will harden much more rapidly and would require the dome to be intermittently heat treated in order to allow for the necessary sinking of higher-range instruments. Low-carbon steel does not require annealing during sinking but the pan head, with final note patterning, is heated or tempered prior to tuning. This provides some sort of stress (strain) relief or homogenization and strain aging which in most cases hardens the notes slightly while stabilizing existing dislocation structures [5].

### 3. Experimental issues and procedures

#### 3.1. Pan construction and tuning

Pans for use as musical pan platforms were individually fabricated in this research program using a Solid Hoop<sup>TM</sup> construction process. These hoops, solid, 9 mm  $\times$  9 mm square low-carbon steel were welded to the pan head and the skirt or sidewall cylinder and form a continuous, rigid joint. The low-carbon steel (standard) pan head was 1.14 mm thick and had a composition (in weight percent) of 0.06% C, 0.22% Mn and the balance Fe. The sidewall was 20 gauge low-carbon sheet (nominally 0.03 in. or 0.8 mm thick) with a composition of 0.09% C, 0.38% Mn and the balance Fe. This sidewall material was used for both the low-carbon steelpan head and the brass pan heads. The brass pan head was 1.24 mm thick, soft Revere C26000  $\alpha$ -brass sheet and had a composition of 69.1% Cu and 30.9% Zn. Table I pro-

vides a comparison of the properties for the low-carbon steel and 70/30  $\alpha$ -brass pan head material, including the initial grain size and Vickers microhardness.

The fabricated pans were 23.5 in. (59.7 cm) in diameter and the heads were domed downward to produce a standard, approximately, semi-hemispherical platform using a pneumatic hammer. The dome depth was  $\sim$ 8.8 in. (22.3 cm) from the pan horizontal (top), and an ultrasonic thickness gauge (Krautkramer (CL3 DL)) was used to measure the dome thickness along reference lines extending from the rim to the pan bottom center. Murr *et al.* [1] have shown that the dome sheet thickness for tenor pans varied from roughly 10% near the rim to 45% of the original sheet thickness at the bottom of the dome. In this study the dome thickness varied in a similar manner although the dome platform was patterned with notes corresponding to a D-lead as shown schematically in Fig. 2a.

The low-carbon steel pan standard was constructed in the way most Caribbean steelpans are constructed, except that the pan was actually fabricated as described above and there were no grooves around the note zones, which is facilitated by the larger platform and which allows for more internote space and more appropriately sized notes. Small guide holes were drilled to mark the major and minor axes references. The skirt length was cut to measure 5 in (12.7 cm) ( $L$  in Equation 7 and illustrated in Fig. 1a). Small (1.5 mm diameter) holes were bored in each note zone border where grooving would traditionally occur (Fig. 1a) to mark the major and minor note axes. The pan was tempered at 288°C for 5 min and notes optimized and tuned.

Three brass pans with low-carbon steel skirts or sidewalls measuring the same length ( $L = 5$  in (12.7 cm) as the low-carbon steel standard were constructed. The first brass pan was completely experimental since it work hardened rapidly and was heated at roughly 550°F (288°C) for 1 h in order to complete the doming process. The dome thickness for the first (experimental) brass pan was similar to the low-carbon steel standard but the low-range (low frequency) notes at the pan rim were soft (from overheating) from a tuning perspective and the tuning was altered somewhat. No variance in the note size (Equation 6) was undertaken and the standard D-lead notes (Fig. 2a) were turned to one-third of the octave range as illustrated in Fig. 2b. Just prior to tuning, the pan was annealed in the same way the low-carbon steel standard pan was annealed (or tempered):  $\sim$ 288°C for 5 min. A second  $\alpha$ -brass pan was similarly fabricated and patterned with notes but although it was sunk to the required shape and depth the brazed joint between the brass dome and the

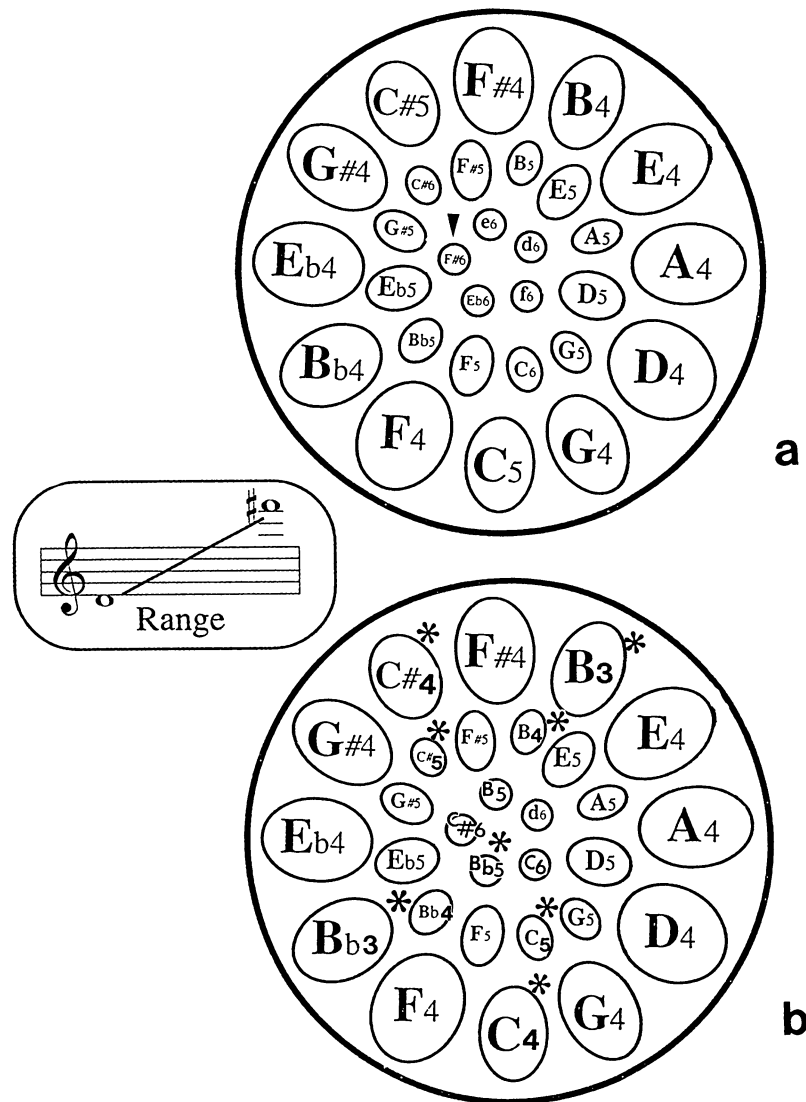


Figure 2 D-lead (soprano range) note patterns characteristic of the low-carbon steel (standard) and a similarly patterned  $\alpha$ -brass pan (pan 3 with  $F_6\#$  absent as indicated by arrow) (a); and the first  $\alpha$ -brass pan (b). The asterisks (\*) in (b) are indicative of the altered tonics from the standard pattern in (a). The tonal range for the standard D-lead is shown in the insert ( $D_4$ (294 Hz) to  $F\#_6$  (1480 Hz)).

hoop failed, and it was used for analysis by cutting it in half, measuring the dome thickness, and cutting out coupons for metallurgical investigation. A third brass pan was fabricated using an altered annealing treatment consisting of firing the dome at roughly  $320^\circ\text{C}$  for 10 min instead of 1 h. The note sizes in the patterned D-lead note zones of this pan were reduced by between 10 and 15% (Equation 6) from the low-carbon steel standard, and these notes were tuned to standard octave ranges noted in Fig. 2a, with the exception of  $F_6\#$  which was eliminated. Prior to tuning, the pan was annealed at roughly  $288^\circ\text{C}$  for 5 min, part of the note optimization.

Since the actual coupling between the note platform and the skirt is weak, the skirt material was not changed for the  $\alpha$ -brass pans and remained the low-carbon (0.09% C) steel sheet. The dimensions, etc. were also unchanged and consequently the frequency range for the skirt (Equation 7) was the same for all pans. Fig. 3 illustrates the low-carbon steel standard pan and the two  $\alpha$ -brass pans constructed and tuned in this research program as described above; along with the failed  $\alpha$ -brass pan which was used for analytical purposes (Fig. 3e and f).

### 3.2. Microscopy and microhardness measurements

The microstructures—grain structure and sub-grain structures—of the various pan materials were examined by both optical metallography and transmission electron microscopy. The initial, low-carbon steel sheet was cut into small coupons, cold mounted, polished to  $0.3\ \mu\text{m}$  mirror finish with a diamond paste, and etched with a nital solution ( $\sim 97\%$  methanol and  $3\%$  nitric acid) after cooling the polished specimens to  $\sim 10^\circ\text{C}$ . Sheet samples were also rolled 20 and 40% (35% for the low-carbon steel because of its starting thickness) to simulate the deformation associated with the domed pan head and coupons cut from these deformed samples similarly prepared. Optical metallography examination was performed on a Reichert MEF4 A/M instrument. Vickers microhardness measurements were also performed on the polished specimens in a Shimadzu HMV-2000 digital microhardness tester using a 100 gf ( $\sim 1\ \text{N}$ ) load for 15 sec/indentation. A similar procedure was employed for the brass sheet except the brass samples were etched in a solution consisting of 50 mL distilled water, 40 mL (3%) hydrogen

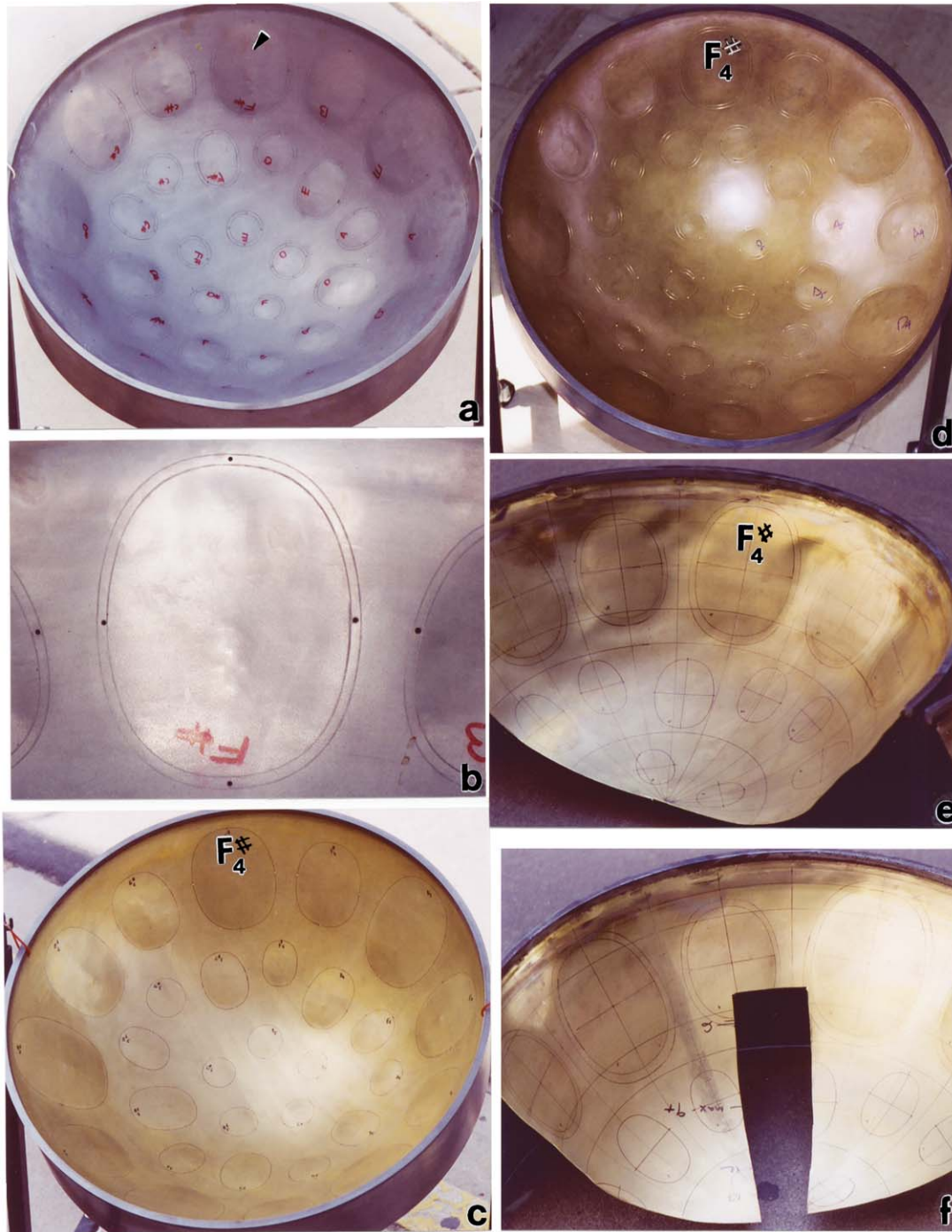


Figure 3 Experimental, D-lead pans fabricated in this research program. (a) Low-carbon steapan standard. (b) Enlarged F#4 note (arrow in (a)). (c) First  $\alpha$ -brass pan turned as indicated in Fig. 2b. (d) Third  $\alpha$ -brass pan with reduced note sizes and tuned as indicated in Fig. 2a with the elimination of F<sub>6</sub>#. (e) and (f) show two halves of the second  $\alpha$ -brass pan which failed at the rim during note zone patterning from which test strips and coupons were extracted (f).

peroxide, and 90 mL ammonium hydroxide chilled to  $\sim 10^{\circ}\text{C}$  in an ice bath. Brass sheet samples were also rolled to 20 and 40% reductions and samples prepared of these materials for both optical metallography and microhardness testing. Coupons were also cut from a domed brass pan at various locations corresponding to the reductions by rolling in order to validate the deformation simulations and examine the actual deformed pan head. Grain size measurements were also made from optical micrographs of both the low-carbon steel and the  $\alpha$ -brass using a simple line intercept method where the average grain intercept length,  $\bar{l}$ , was multiplied by 1.5 to obtain an average grain diameter,  $D$ :

$D = 1.5 \bar{l}$ . Annealing twin boundaries were included in the  $\alpha$ -brass measurements.

A Hitachi H-8000 analytical transmission electron microscope (TEM) fitted with a goniometer-tilt stage was used to examine thin foil, sub-grain microstructures. Sheet samples of both the low-carbon steel and brass, including the deformed sheets and the samples extracted from a domed brass pan head, were cut into small  $\sim 1 \text{ cm}^2$  coupons and ground to  $\sim 0.2 \text{ mm}$  thickness. Standard 3 mm TEM discs were then punched from these thin sections and final polished in a Struers Tenupol 3-dual-jet electropolishing unit. A solution consisting of nominally 0.8 L methanol, 0.2 L ethanol,

0.125 L perchloric acid at  $-20^{\circ}\text{C}$  was used to prepare low-carbon steel thin specimens while a solution consisting of 0.8 L water, 0.4 L ethanol, 0.08 L propanol, 0.35 L phosphoric acid, and 7.5 g of urea (at  $15^{\circ}\text{C}$ ) was used to electropolish thin specimens of the brass.

### 3.3. Acoustic analysis and comparisons

Detailed acoustic spectral analyses were made for common octave ranges on both the low-carbon steel pan standard and the  $\alpha$ -brass pans using an acoustic isolation chamber and a microphone which recorded the sound of notes struck with a standard mallet (neoprene covered hollow aluminum tube). The recorded sounds were analyzed in a Macintosh-compatible computer using Sound Design II and Sound Effects software to resolve time-amplitude pulse spectra and to produce three-dimensional spectral or frequency analysis plots showing frequency, time, and amplitude.

In addition to acoustic measurements on actual drum notes, a series of experiments was conducted on ideal, free circular discs as described in previous experiments on 316 stainless steel [1] and low-carbon steel [5]. For such flat, ( $H_0 = 0$  and  $H_0/h = 0$  in Equation 2) free circular, ideal notes the fundamental frequency is given by [12]

$$f = A(h/a^2) \quad (6a)$$

where  $A = 0.41[E/\rho(1 - \nu^2)]^{1/2}$ . Consistent with previous work, the starting pan head materials (low-carbon steel sheet 1.12 mm thick and  $\alpha$ -brass, 1.24 mm thick) were cold-rolled as noted previously to 20 and 35% reduction (by reverse, multiple-pass rolling), and 20 and 40%, respectively. These rolled plate samples and the original plates were then milled to achieve a thickness of 0.070 to 0.075 cm, and circular discs 3.7 cm in radius were then cut from the low-carbon steel samples. In order to maintain the same (or approximate) fundamental frequency (Equation 6a; Table I) the circular discs from the  $\alpha$ -brass samples were cut to a 3.2 cm radius. In addition, to correlate the low-carbon steel and  $\alpha$ -brass pan materials with the earlier stainless steel results [1], and to examine an additional candidate pan alloy, a 316L stainless steel plate 1.25 mm in thickness (with a composition of 16.4% Cr, 10.2% Ni, 2.1% Mo, 0.35% Si, 1.0% Mn, 0.02% C; balance Fe by weight) was cold-rolled in the same manner as the  $\alpha$ -brass to 20% and 40% reduction. The 316L stainless steel had an elastic modulus ( $E$ ) of 195 GPa,  $\nu \cong 0.28$ , and  $\rho = 7.9 \text{ Mg/m}^3$ . Microhardness measurements were also made for the 316L stainless steel samples (corresponding to 0%, 20%, and 40% reduction; using a 300 gf ( $\sim 3 \text{ N}$ ) load). Circular discs identical to those for the low-carbon steel ( $a = 3.7 \text{ cm}$  and  $h \cong 0.073 \text{ cm}$ ) were cut from the 316L stainless steel samples. A 1-mm hole was drilled in each circular disc 1 mm from the edge and hung with a 28-gauge steel wire loop to record the acoustic spectrum when struck with a wooden mallet.

## 4. Results and discussion

### 4.1. Microstructures and related metallurgical issues

Figs 4 and 5 show the grain structure and the sub-grain microstructures for the starting low-carbon steel dome sheet and the same sheet cold-rolled (reduced) by 35% in comparison with the starting  $\alpha$ -brass dome sheet, and the same sheet cold rolled to 40% reduction, respectively. The low-carbon steel pan sheet (Fig. 4a) exhibits an essentially equiaxed grain structure with an average grain size of  $20 \mu\text{m}$ , and a Vickers hardness of 118 VHN (1.18 GPa); consistent with low-carbon steel sheet (or pan lid) grain sizes ranging from 16 to  $34 \mu\text{m}$  and Vickers hardness variations from 113 to 139 VHN measured in earlier work by Ferreyra *et al.* [2]. The FCC  $\alpha$ -brass grain structure shown in Fig. 4c and d was also essentially equiaxed and contained numerous annealing twin boundaries; with an average grain size of  $30 \mu\text{m}$ . The 40% rolled sample shown in Fig. 4d exhibits planar (but distorted) deformation features characteristic of microtwin faults on the  $\{111\}$  planes and stacking faults which are a result of the low-stacking fault free energy for  $\alpha$ -brass [13]. These linear or planar defect features are illustrated in Fig. 5c in contrast to the more irregular dislocation substructure characteristic of the BCC (ferritic) low-carbon steel shown for comparison in Fig. 5a and b. Fig. 5d shows dense dislocation substructure in comparison to the starting sheet shown in Fig. 5c.

It can be noted in Fig. 5 that the initial dislocation densities (Fig. 5a and c) are roughly  $10^9 \text{ cm}^{-2}$ , with the low-carbon steel exhibiting a slightly higher dislocation density than the  $\alpha$ -brass. The dislocation density increases by roughly an order of magnitude when cold-rolled 35% for the low-carbon steel, and 40% for the  $\alpha$ -brass as shown on comparing Fig. 5a–d, respectively.

Fig. 6 shows for comparison a few, representative measurements of per cent thickness reduction throughout the low-carbon steel (standard) pan head (Fig. 3a) and the failed  $\alpha$ -brass pan head (Fig. 3e and f) using the ultrasonic thickness gauge. The  $\alpha$ -brass pan head thickness reductions were also measured directly from the half-section shown in Fig. 3f using a micrometer, and these data act as a calibration for the corresponding ultrasonic thickness (% reduction) measurements in Fig. 6. The data plotted in Fig. 6 attest to the overall accuracy of ultrasonic thickness measurements for both the low-carbon steel and  $\alpha$ -brass pan heads as well as the uniformity and reproducibility in the D-lead pan fabrication, especially the pan head doming. The data in Fig. 6 are also generally consistent with the original pan head cross-section (thickness reduction) measurements of Murr *et al.* [1] for steelpan construction from 55-gallon steel barrels.

Fig. 7 shows a plot of the average Vickers microhardness for the cold roll-reduced low-carbon steel and  $\alpha$ -brass pan head sheet and the corresponding microhardness averages for coupons extracted from the failed  $\alpha$ -brass pan as shown in Fig. 3e. The actual  $\alpha$ -brass pan head thickness reductions in Fig. 7 are somewhat lower than the corresponding cold roll-reduced  $\alpha$ -brass

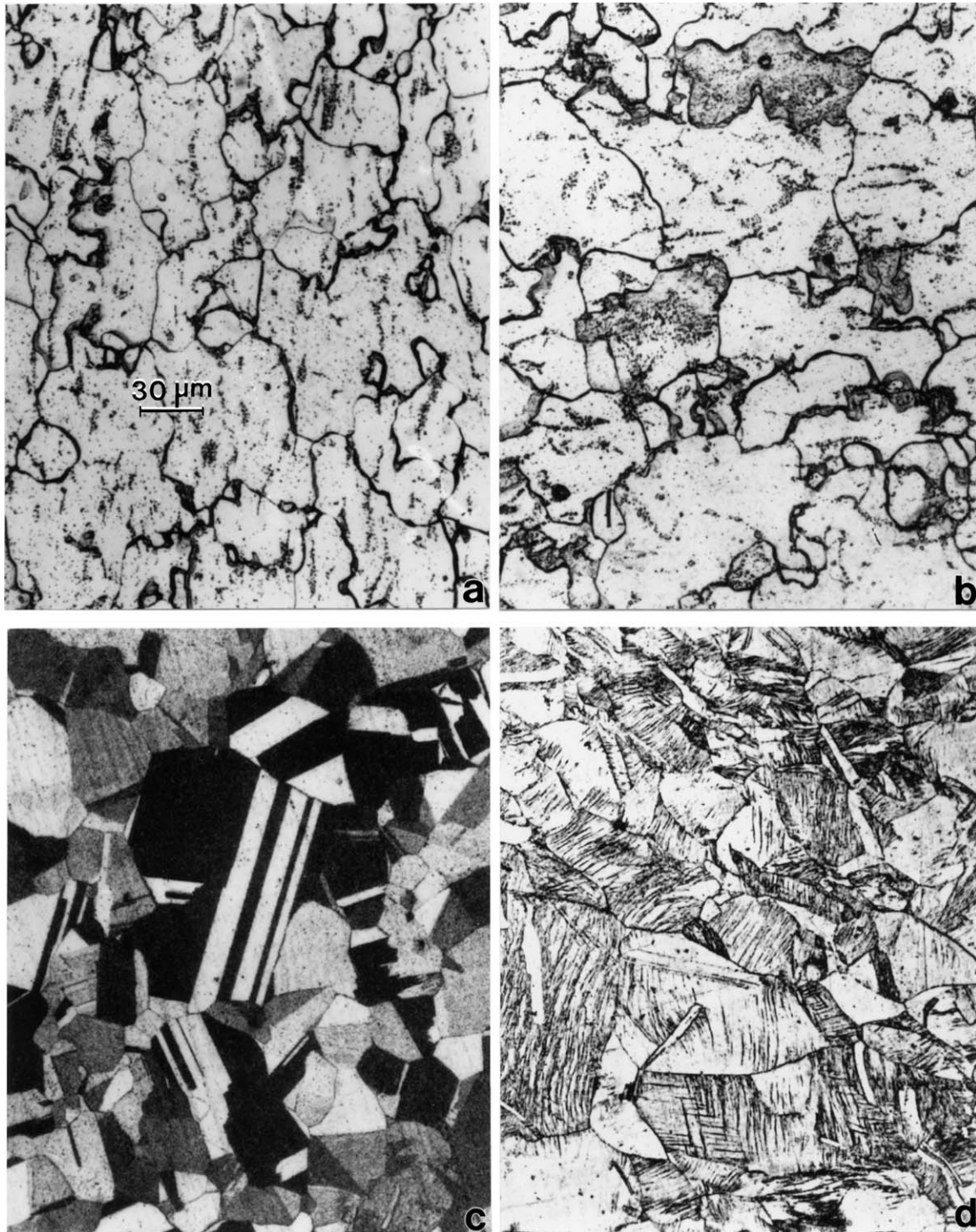


Figure 4 Optical micrographs showing original, starting pan head grain structures and the same structures after cold reduction. (a) Original low-carbon steel sheet. (b) Low-carbon steel sheet cold-rolled 35%. (c) Original  $\alpha$ -brass sheet. (d)  $\alpha$ -brass sheet cold-rolled 40%. Note distorted, planar defects in the grains. Magnifications for all figures are the same as shown in (a).

starting sheet, in part because of the strain-state variation in the deformed pan dome by pneumatic hammering to shape it and a slight reduction in hardness due to the heat treatment during doming. Nonetheless, the maximum hardness values are comparable near the bottom of the  $\alpha$ -brass pan (Fig. 6) and the microstructures are correspondingly similar as illustrated in the optical and TEM images shown for comparison in Fig. 8. Fig. 8a shows deformation features similar to those in the 40% roll-reduced  $\alpha$ -brass sample shown in Fig. 4d while Fig. 8b illustrates the corresponding and similar deformation microstructure view in the

pan thickness, at roughly 40% reduction in the dome thickness (Fig. 6). Fig. 8c shows for comparison a TEM microstructure image for the  $\alpha$ -brass pan region shown in Fig. 8a and corresponding to a distance of roughly 15 cm from the pan rim in Fig. 6. Fig. 8d shows a similar TEM image of the  $\alpha$ -brass microstructure at a distance of roughly 23 cm from the pan rim in Fig. 6 which is similar to Fig. 8c. Both Fig. 8c and d contain microtwin faults which are indicated by the corresponding  $\langle 111 \rangle/3$  twin reflections noted by the arrows in the selected-area electron diffraction pattern inserts. The microstructures in Fig. 4d are not noticeably different, and represent



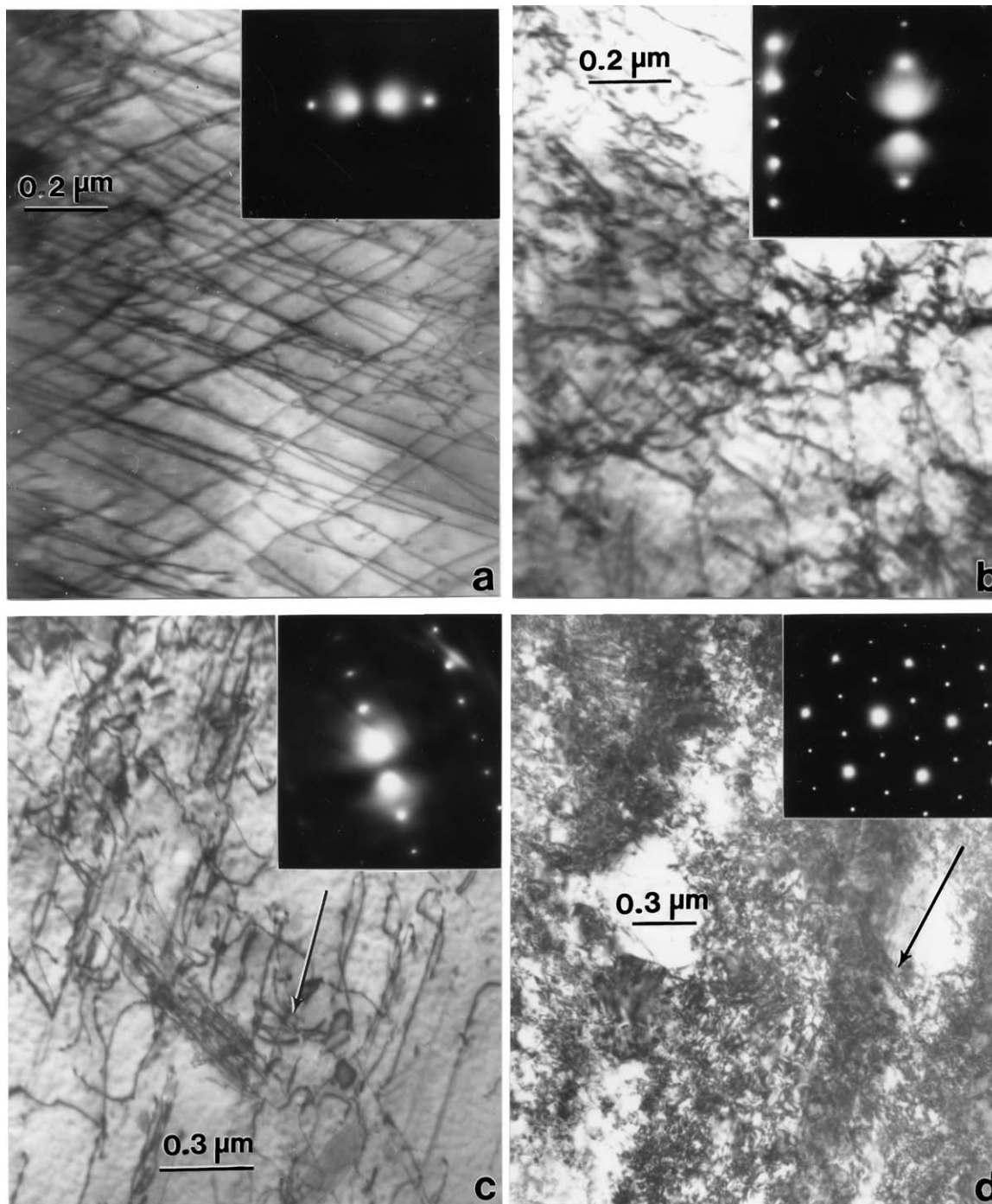


Figure 5 TEM bright-field images showing sub-grain microstructures in the experimental pan head materials corresponding to Fig. 4. (a) Original low-carbon steel. (b) Low-carbon steel cold-rolled 35%. Selected-area electron diffraction pattern inserts show (112) and (111) grain surface orientation for (a) and (b) respectively. The operating reflection is the same ( $[1\bar{1}0]$ ) in each case. Systematic reflections are absent in the patterns because of buckling of the foil. (c) Original  $\alpha$ -brass. (d)  $\alpha$ -brass cold-rolled 40%. Selected-area electron diffraction pattern inserts show (110) grain surface orientations. Arrows represent the  $[1\bar{1}0]$  direction.

$\alpha$ -brass sheet thickness reductions (or corresponding plastic strains) ranging from roughly 40 to 50%. Note in comparing Figs 5d, 8c and d that the grain surface orientations are the same (110) orientations shown by the selected-area electron diffraction pattern inserts. Based upon prior observations of actual low-carbon steel pan microstructures [1, 2], it might be expected that similar features would be characteristic of the low-carbon steel pan microstructures for Fig. 3a. It is also of interest to note that the hardness profiles for the cold-reduced  $\alpha$ -brass and the low-carbon steel in Fig. 7 are the same, and the maximum low-carbon steel hardness at 35% thickness reduction ( $\sim 170$  VHN) is essentially equiv-

alent to the maximum hardness obtained after the final, short heat treatment for the more common 55-gallon barrel steel pans in the previous studies of Ferreyra *et al.* [2].

It is of interest to note that while there is a difference in dislocation substructures in the more heavily deformed (BCC) low-carbon steel sheet and the (FCC)  $\alpha$ -brass pans, and rolled sheet (Figs 5b, 5d, 8c and d), the corresponding hardnesses are similar and the residual pan note stabilities (or rigidities) would be assumed to be similar. However, in contrast to the low-carbon steel, the  $\alpha$ -brass dome required heat treatment in order to complete the doming process in large part due to the

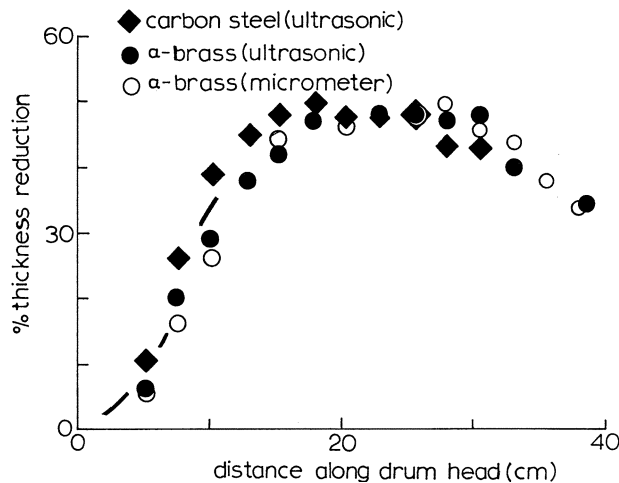


Figure 6 Per cent reduction versus distance along the pan head measured from the pan rim at zero. The carbon steel measurements are for the experimental pan in Fig. 3a. The  $\alpha$ -brass measurements are for the experimental pan in Fig. 3d and e.

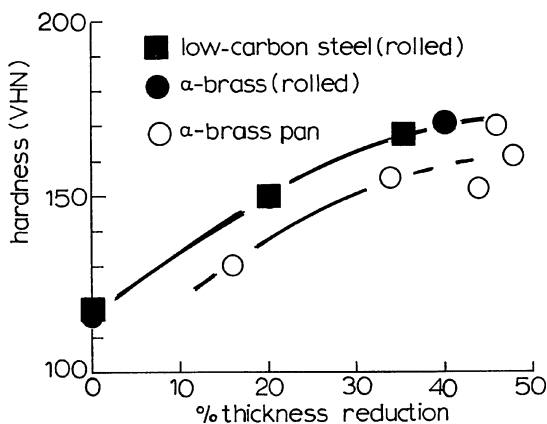


Figure 7 Vickers hardness (VHN) versus per cent reduction for the cold-rolled pan head sheet materials and for coupons extracted from the experimental  $\alpha$ -brass pan shown in Fig. 3d and e.

fact that the work-hardening in the  $\alpha$ -brass was twice that for the low-carbon steel (see Table I). This heat treatment, while primarily a mild stress relief anneal, must be adjusted to maintain requisite note stability in order to be conveniently tuned. In other words, the pan head needs to be as hard as possible without imposing difficulties in tuning. Moreover, the heat treatment at the conclusion of doming or forming of the pan head and prior to tuning, which was maintained for the  $\alpha$ -brass as well as the low-carbon steel pan, seemed to serve only as a final, stress homogenization in the  $\alpha$ -brass since there is no strain aging as in the low-carbon steel [2, 5]. In fact, it is unclear that this heat treatment step was at all necessary in the  $\alpha$ -brass pan fabrication.

#### 4.2. Acoustic analysis and tuning issues

Fig. 9 shows for comparison the sound pulse spectra or amplitude-time signals corresponding to each of the sample discs (free, circular notes having a constant thickness,  $h \cong 0.073$  cm) along with their Vickers hardness values (VHN). Because of the variations in

the disc thicknesses the fundamental frequencies varied by as much as 15%. For example,  $f \cong 1400$  Hz for the 316L stainless steel;  $f \cong 1250$  Hz for the low-carbon steel;  $f \cong 1180$  Hz for the  $\alpha$ -brass discs. These signal data exhibit a consistent effect of deformation and the 316L stainless steel results are essentially the same as those illustrated previously [1]. It should be apparent that aside from the adjusted radius for the  $\alpha$ -brass discs, the samples differ only in the deformation-induced microstructures corresponding to 20 and 35% or 40% reduction, and the extremes (0 and 35% or 40%) are illustrated by the deformation microstructures in Figs 4, 5 and 8 for the low-carbon steel and the  $\alpha$ -brass. The 316L stainless steel microstructures were similar to those illustrated previously [1]. While the specific acoustic phenomenon may not have any musical significance, it is apparent in Fig. 9 that deformation-induced microstructures (especially dislocation density) affect the sound pulse in the same, systematic way.

Even more interesting is the observation, shown typically in Fig. 10, that the sound pulse shape change shown in Fig. 9 for ideal, flat, free-circular notes are also observed to some extent in the actual pan notes. Of course, unlike the ideal notes in Fig. 9b and c respectively for the low-carbon steel and  $\alpha$ -brass, the  $D_4$ ,  $D_5$ , and  $D_6$  notes in the corresponding pans are more complex because these octave ranges are characterized by changing note size ( $a$ ), thickness ( $h$ ), and rise ( $H_0$ ); Fig. 1b and Equations 2, 4–6; in addition to variations in deformation or dome thickness reductions which range from roughly 20 to 30% for  $D_4$  to 40 to 50% for the  $D_5$  and  $D_6$  notes. These features are also apparent in the tenor pan Vickers hardness maps constructed in the previous work of Ferreyra *et al.* [2]. It should be noted that the ideal circular note frequencies (Fig. 9) corresponded approximately to  $D_6$  ( $\sim 1175$  Hz) for the  $\alpha$ -brass,  $D_6^\#$  ( $\sim 1245$  Hz) for the low-carbon steel, and  $F_6$  ( $\sim 1397$  Hz) for the 316L stainless steel; all at the pan head bottoms (Fig. 2). It is also observed in Fig. 10 that the two brass pans have a slightly different pulse shape for each note in contrast to the carbon-steel standard. This reflects a different pan timbre and is due in part to note differences or the need to shape the brass differently from the carbon steel. This is in part a reflection of the refinement for carbon steel pans over many years in contrast to only two experimental brass pans in this research program.

It should be noted that while we have emphasized a different note geometry (size) for the brass pans, it is possible to attain similar modulations in any pan note by varying the note rise,  $H_0$ , as shown in Equation 2; especially by increasing the note size for the  $\alpha$ -brass pans.

All the vibrators (flat discs and domed notes) in this study are dynamically non-linear devices. In the dynamics of the flat discs there are cubic non-linearities while for the domed shells there are both quadratic and cubic non-linearities. When excited into vibrational motion, these vibrators produce, in addition to the normal modes (as studied in this paper), low-level parametric excitations. These excitations may allow

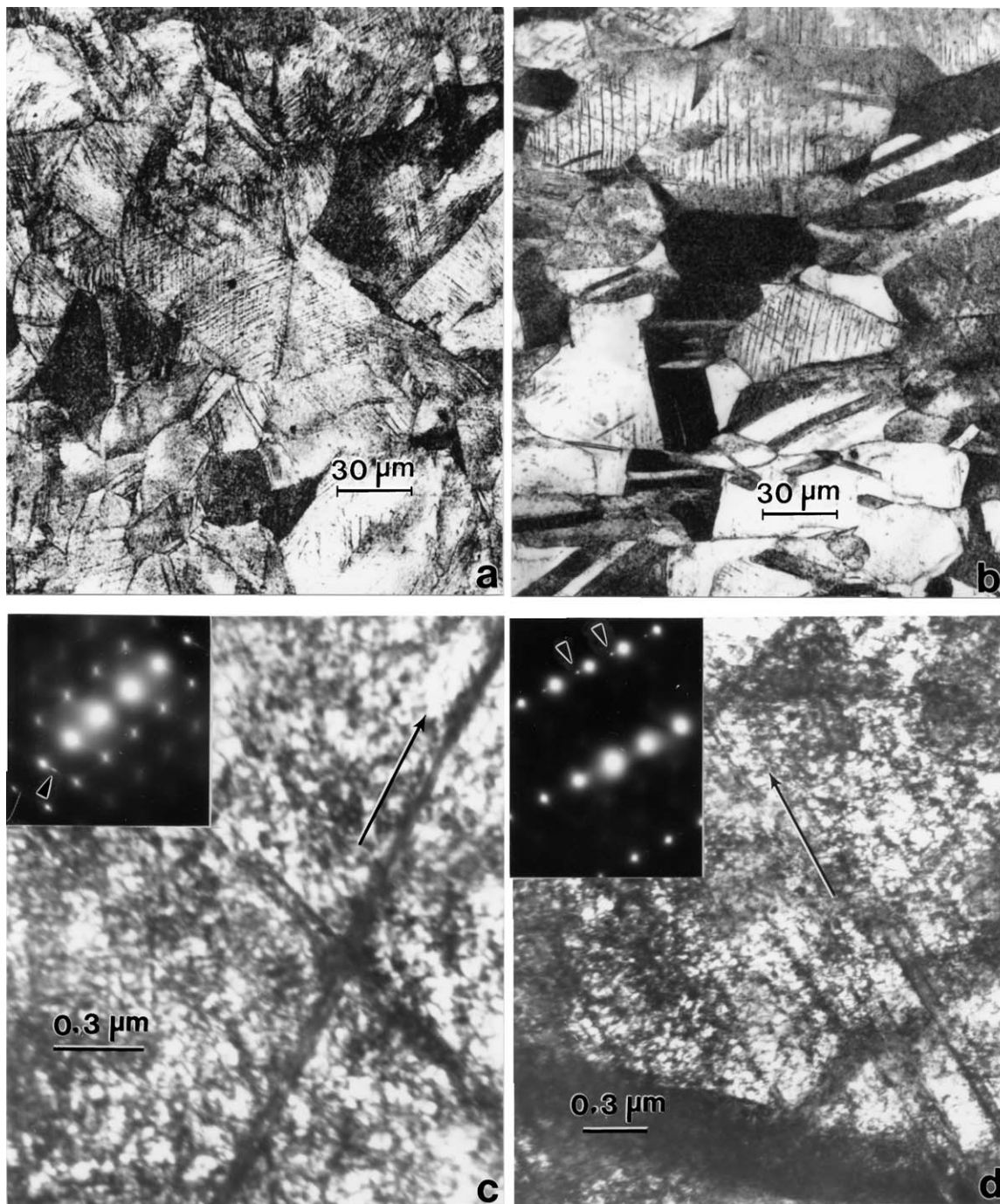


**Figure 8** Optical and TEM micrographs of  $\alpha$ -brass coupons extracted from the pan in Fig. 3d and e. (a) Deformed sample in the plane of the pan corresponding to a distance of  $\sim 15$  cm ( $\sim 43\%$  reduction) in Fig. 6. (b) Deformed sample coupon in (a) in the thickness direction (at  $90^\circ$  to (a)). (c) TEM image corresponding to (a). Selected-area electron diffraction pattern insert shows (110) grain orientation. Twin reflection  $((111)/3)$  perpendicular to the  $[1\bar{1}2]$  microtwin trace direction shown by the long arrow in the image is marked by small arrow in the pattern. (d) TEM image for a coupon extracted at a distance of  $\sim 23$  cm (Fig. 6) from the pan rim in Fig. 3e. Twin reflections  $((111)/3)$  perpendicular to microtwin faculae along  $[1\bar{1}2]$  (large arrow in the image) are marked by small arrows in the (110) selected-area electron diffraction pattern insert. Systematic reflections in the pattern are absent because of foil buckling.

the normal modes to interact (couple) via parametric internal resonances depending on the linear frequencies of the higher modes. This results in amplitude and frequency modulations of the normal modes and also the “delayed overtones” (Figs 9 and 10). The degree of mode coupling produced through these internal resonances depend on the material properties and in particular the geometry in the case of the quadratic effects. The plots of Figs 9 and 10 are classic examples of these effects as identified in their references. The complexity of the pulse shapes is due to

internal resonances that in turn depend on the closeness of the “octaves” to the harmonics of the fundamental. This is because the parametric excitations (save for some small detuning) are at the harmonics of the fundamental (the major ones, for there are also non-linearly produced mixed modes having sum and difference frequencies). The “variations in complexity” and not the “complexity” itself are due to changing geometrical parameters ( $a$ ,  $h$ ,  $H_0$ ) as mentioned above. Changes in just the form (geometry) alone (leaving all else unchanged) can bring about

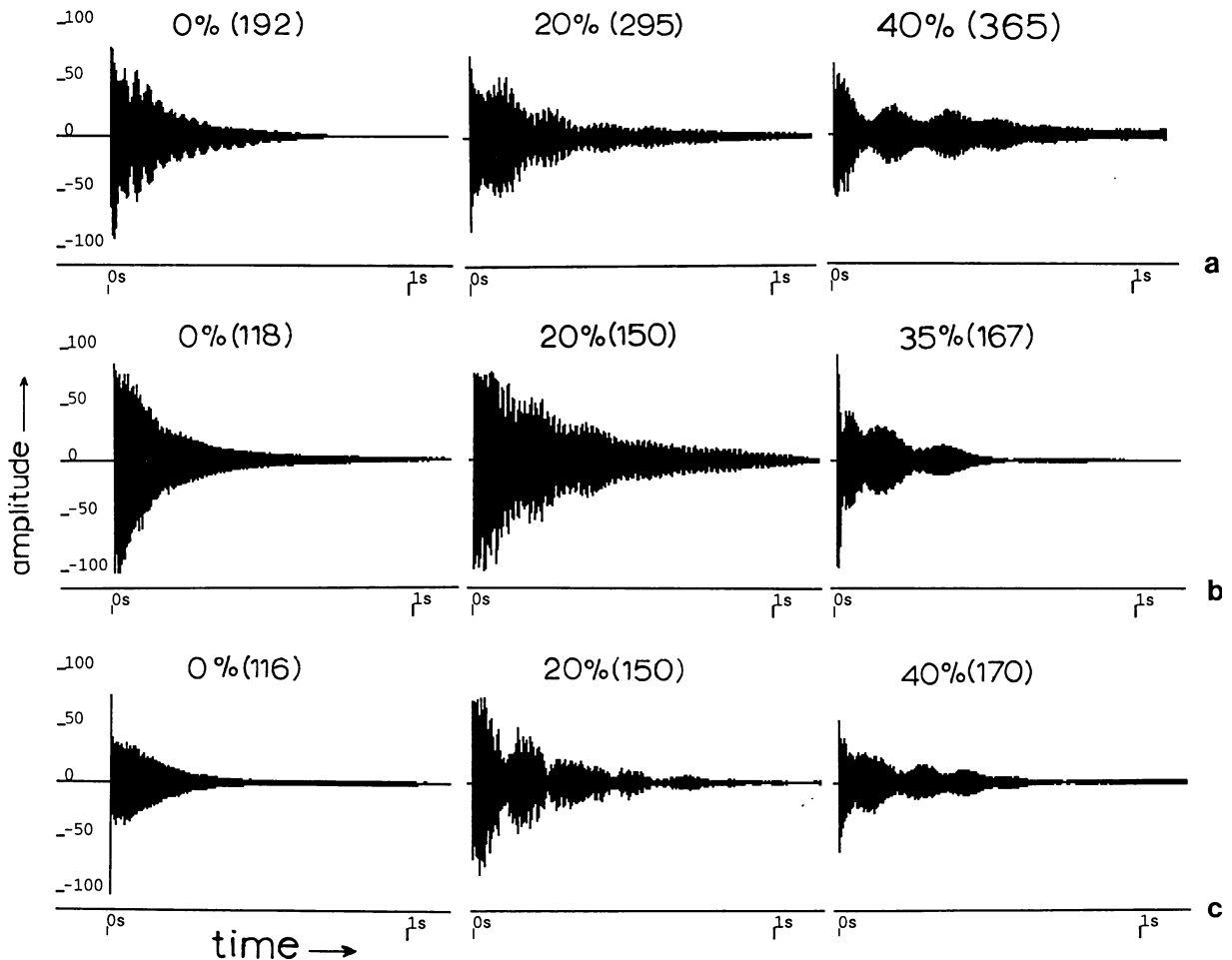


Figure 9 Sound pulse spectra (amplitude versus time) for free circular disc notes corresponding to cold reductions (%) noted; with Vickers hardness numbers (VHN). (a) 316L stainless steel. (b) Low-carbon steel (0.06% C). (c)  $\alpha$ -brass.

very noticeable (and audible) changes in the profiles of Fig. 10.

While it is difficult to convey issues which relate directly to the sound of notes, or differences in the sound of the same notes on different pans, as illustrated in the impulse responses compared in Figs 9 and 10, three-dimensional sound spectra can provide a more graphic representation. To graphically describe a sound, the frequency content or frequency spectrum changes with amplitude (or energy in decibels) and time must be investigated. Fig. 11 shows several three-dimensional (time-amplitude (or energy)-frequency) plots corresponding to the impulse (amplitude-time) spectra shown in Fig. 9 for the 316L stainless steel and the  $\alpha$ -brass; at 0% rolling reduction and 40% reduction. While the similarities of the frequency spectra are indicative of the consistency of the disc geometries, there are also differences in modes observed at 0% in contrast to those at 40%. In previous work involving 316 stainless steel discs, single modes seemed to split in response to the deformation or roll-reduction [1]. However these observations involved very short-time modes which are not observed in Fig. 11. Moreover, such sound effects would not be audible, and would not be of any practical consequence. It is interesting to note that in common listings of the longitudinal sound velocity [14], the value changes depending upon whether the material is annealed or deformed. For example, common

handbook values for annealed and rolled copper are  $4760 \text{ ms}^{-1}$  and  $5010 \text{ ms}^{-1}$  respectively while for annealed and drawn tungsten the values are  $5220 \text{ ms}^{-1}$  and  $5410 \text{ ms}^{-1}$  respectively. While tungsten is certainly not a candidate for a pan, the fact that the sound velocity changes with deformation is interesting in light of the fact that tungsten is the only truly isotropic metal, i.e. its elastic modulus of 411 GPa is not altered by crystallographic direction, texturing, etc. In this regard, Ferreyra *et al.* [5] have shown that there is no significant texturing in either low-carbon steel pans or in 316 stainless steel similarly deformed, and the elastic modulus does not change by more than  $\sim 2$  per cent. However, the effective, higher-order elastic constants are sensitive to microstructure (deformation), and it may be these higher-order phenomena which are responsible for what appear to be acoustic anomalies in Fig. 9. However these “anomalies” can be fully accounted for in terms of non-linear mode coupling. In spite of these issues, there do not appear to be any prominent acoustic consequences of the pan microstructures except of course the fact that the microstructures, such as those illustrated in Figs 5, 8c and d, are the agents for strength and hardness which provide for tuning and note stability. When these microstructures are annealed out or significantly altered by excessive, localized heating of a note, there is no recourse, and the note cannot be tuned. That is, it is not possible to locally deform the note

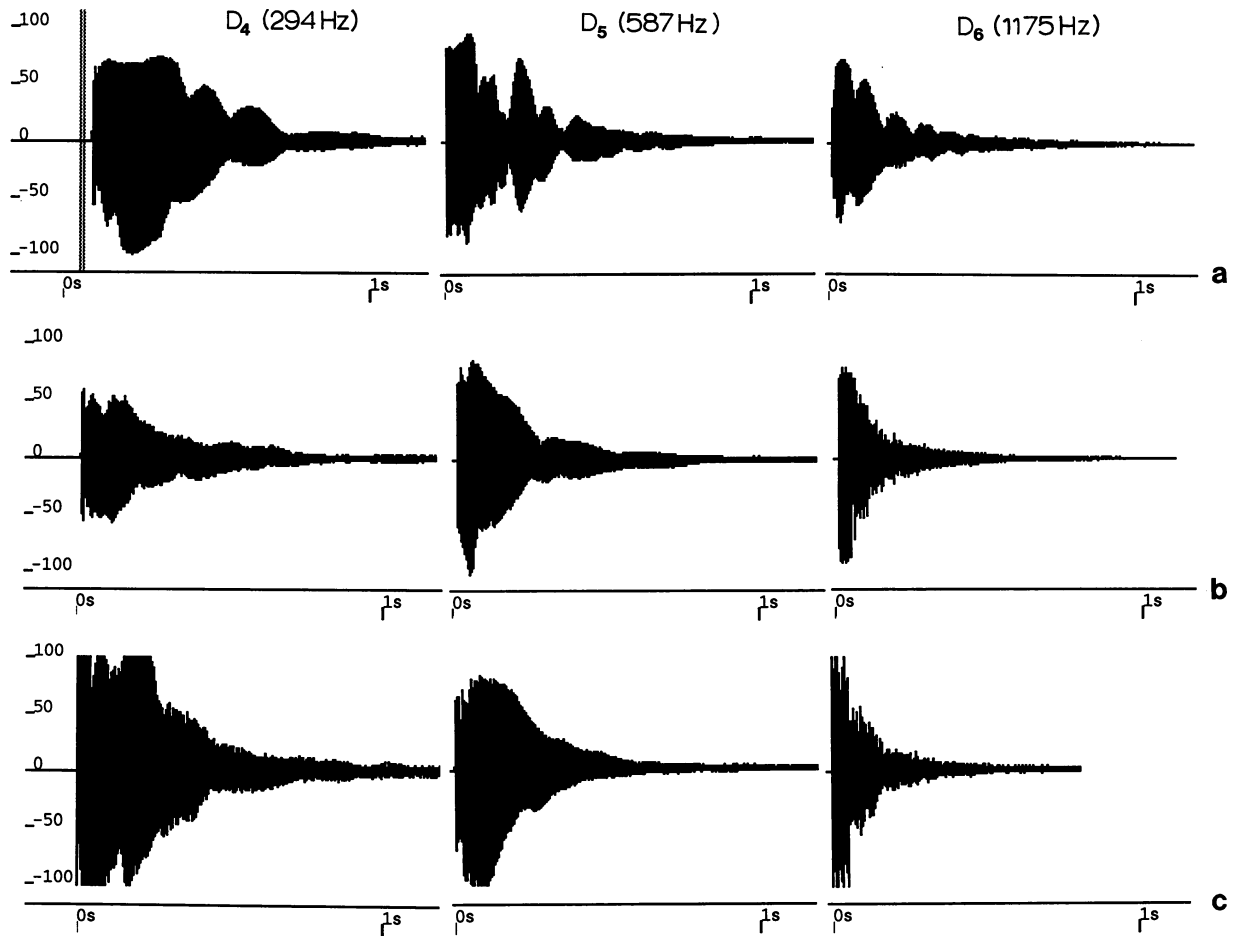


Figure 10 Sound pulse spectra (amplitude versus time) for  $D_4$ ,  $D_5$  and  $D_6$  common to the low-carbon steelpan standard and the two tuned  $\alpha$ -brass pans. (a) Low-carbon steelpan standard. (b) First  $\alpha$ -brass pan tuned as in Fig. 2b. (c) Third  $\alpha$ -brass pan tuned as in Fig. 2a for the low-carbon steel pan except for the elimination of  $F_6\#$ .

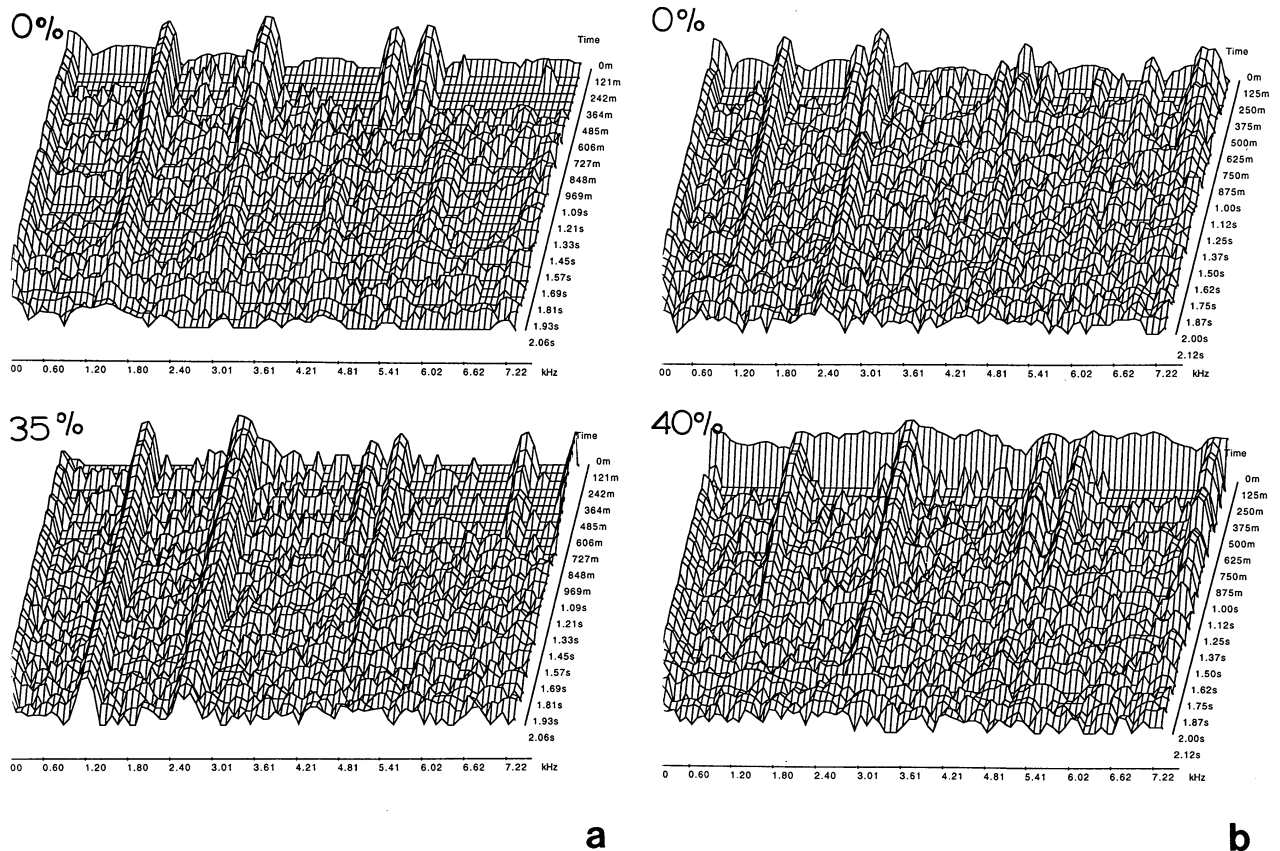


Figure 11 Three-dimensional (time-amplitude-frequency) plots for the cold-rolled discs. (a) 316L stainless steel. (b)  $\alpha$ -brass. The corresponding reductions are shown. Times (m) are in milliseconds.

to its original, equivalent hardness and corresponding deformation microstructure. When a properly tuned, pan note is struck, one or more delayed overtones are heard. Truly chromatic tones originate more often in the lower-frequency range, larger-size notes nearest the rim in the higher range instruments. When the mallet strikes a note, the note vibrates at modes above the fundamental, tuned harmonically by the pan tuner, as well as sympathetic vibrations from neighboring notes (Equations 1 and 2). These features are illustrated in the three-dimensional sound plots in Fig. 12 which include the original impulse spectra; and compares these sound data for the  $A_4$  (440 Hz) and  $A_5$  (880 Hz) notes on the low-carbon steel standard pan and the two  $\alpha$ -brass pans (compare Fig. 2a and b respectively). These graphics illustrate the similarities of the notes for these different pans as well as their differences, particularly their tonal or chromatic differences. The low-carbon steel standard pan exhibits numerous prominent parametric excitations which appear at nearly exact multiples of the tonic (primary frequency) as noted especially for  $A_4$ .

Correspondingly, only the first octave ( $2f$ ) is prominent in  $A_4$  for the first (flat)  $\alpha$ -brass pan (Fig. 12b) and the third  $\alpha$ -brass pan tuned like the carbon-steel pan except for  $F_{6\#}$  (Fig. 12c). However there are other harmonics, but not as prominent as the carbon steel pan. This feature especially applies to  $A_5$  as well. Consequently, there is a sound difference between  $A_4$  and  $A_5$  for the low-carbon steel pan, and the  $\alpha$ -brass pans as reflected in the spectral plots of Fig. 12. Some listeners would say the  $\alpha$ -brass pans are not as bright in their timbre. Considering that the brass pans constructed in this research program are a first effort compared to at least hundreds of thousands of steel pans made in the world, the similarities are striking. However, these similarities are not unexpected because all the pan versions considered in this study follow identical dynamics, but with each having a unique set of parameters. It is for this reason that the hundreds of thousand of pans made in the world did not affect those constructed for the present study; each is unique in its details.

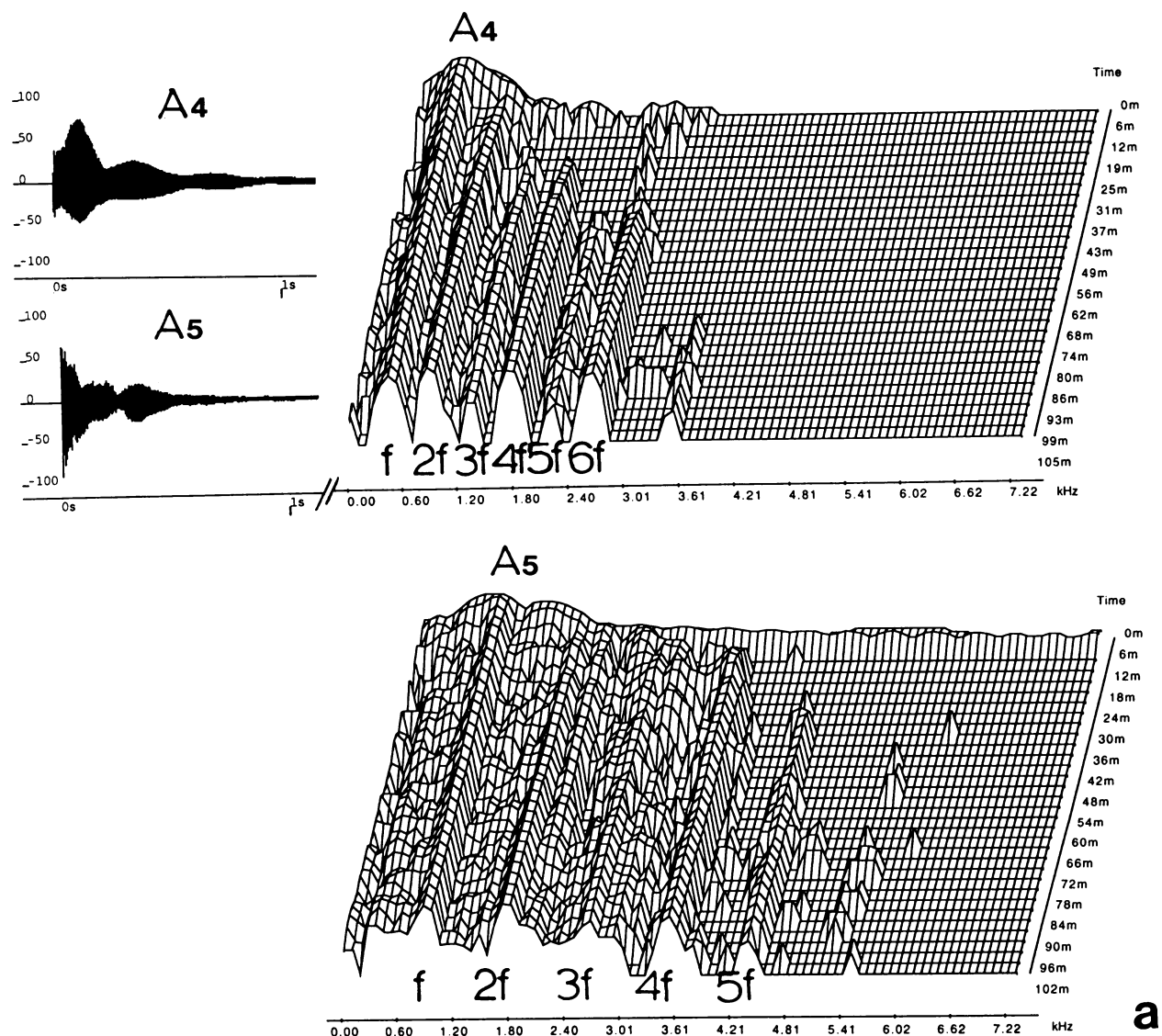


Figure 12 Comparison of three-dimensional (time-amplitude-frequency) plots for  $A_4$  and  $A_5$  notes on the low-carbon steel drum standard (a), the first  $\alpha$ -brass pan (tuned as indicated in Fig. 2b) (b), and the third  $\alpha$ -brass pan (tuned as indicated in Fig. 2b except for  $F_{6\#}$ ) (c). The corresponding amplitude-time impulse spectra are also included. Note times indicated ( $m$ ) are milliseconds. (Continued)

### 4.3. The practical implications of metallurgical issues in pans

For over fifty years musical instruments referred to as the steel pan have been made, as the name implies from steel pans—the 55-gallon drums manufactured for storage and transport of oil (petroleum) and a wide variety of other products [15]. The instruments are traditionally made by manually sinking (with heavy ball-peen hammers) the flat surface of the drum into a concave platform for placing the notes. Low-carbon steelpans were domed or sunk by a variety of mechanized methods, including hydroforming, between 1975 and 1985; especially at the Caribbean Industrial Research Institute (CARIRI) and The University of the West Indies (UWI) in Trinidad. Some of these low-carbon steel hydroformed pans were tuned by master pan builders Anthony Williams and Bertie Marshall as well as other tuners [16], and field tested in the 1976 Panorama competition in Trinidad; and were reported as playing as well as the more traditionally constructed pans. Brass pans, or at least brass pan heads, were fabricated (domed and patterned) by hydroforming, along with other materials such as stainless steel in the mid 1980's for the CARIRI/UWI project in Trinidad, but

there is no published record of the success of tuning and playing brasspans. In addition, there do not appear to be any records of brass pans fabricated in the traditional way as shown in this paper. This historical perspective combined with the current context illustrated herein seems to indicate that pans created by a variety of forming processes can be successfully constructed [17], and once properly formed, tunable instruments can be made from other metals, especially brass (as demonstrated herein), and stainless steels; especially low-carbon stainless steels such as 316L where no strain-induced  $\alpha'$ -martensite will form during fabrication [18].

It should not be surprising that brass can be used to make such an instrument, given that it is the metal of choice for several standard, well-known wind instruments, in which the flared end of the tube (the bell) radiates and controls the sound. There seems to be no reason why hard aluminum alloys should not also make acceptable instruments. We should be all familiar with the harmonious sound we hear in many stores, of wind chimes made from aluminum alloys. In fact there seems to be no reason why other metals (e.g. nickel alloys, titanium and other copper alloys)

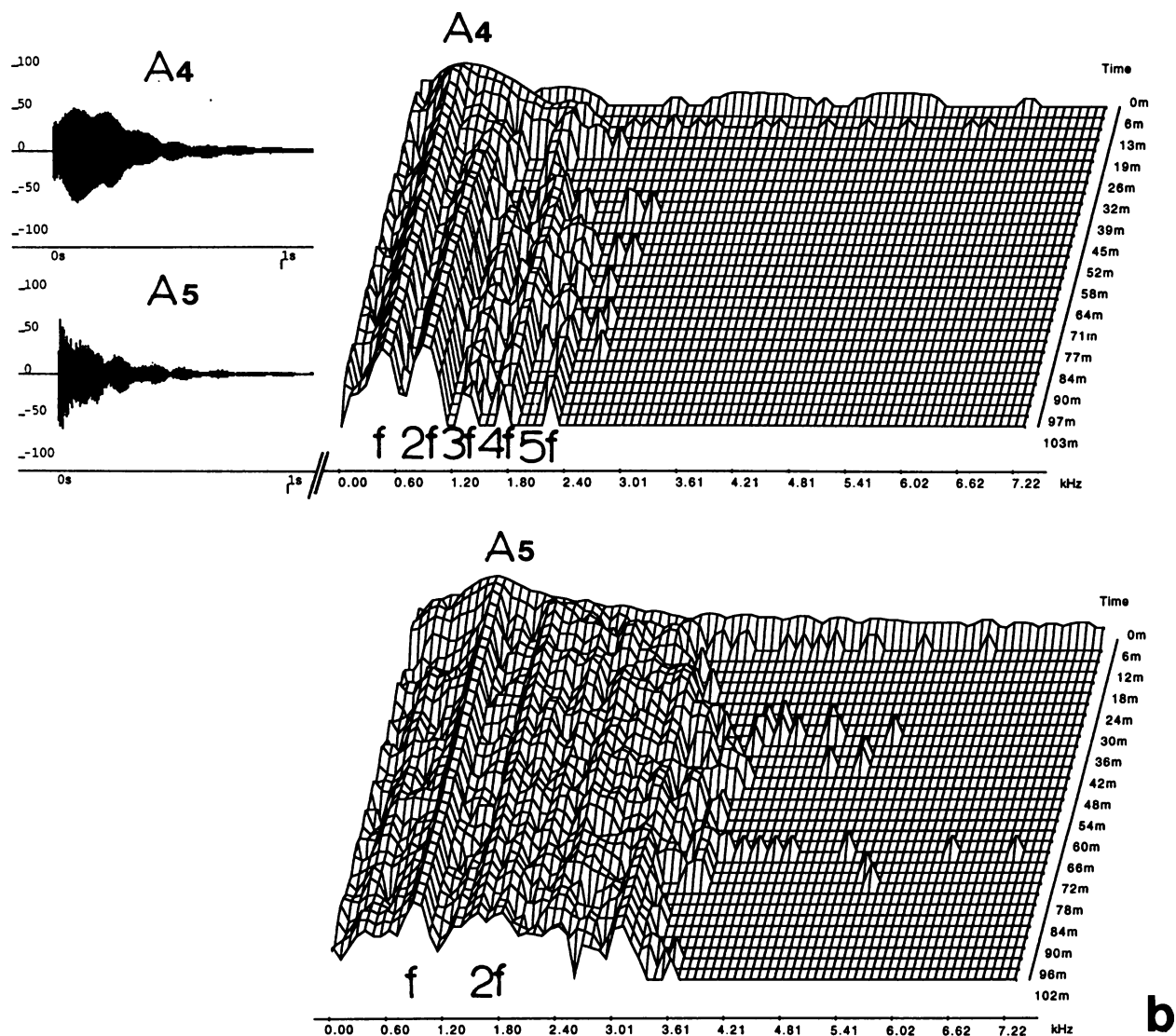


Figure 12 (Continued)

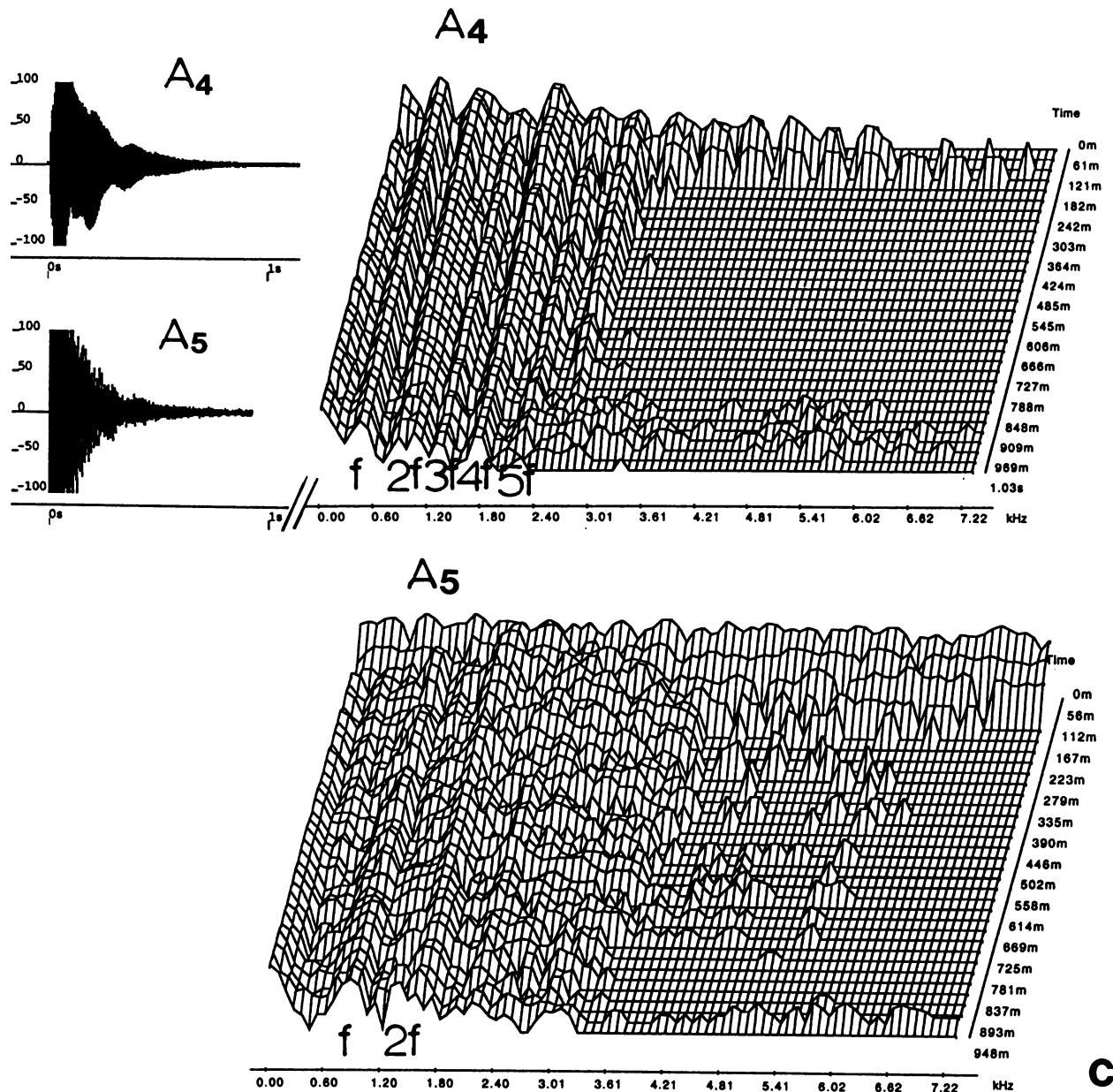


Figure 12 (Continued)

cannot be used to “successfully” make these instruments, success in such matters being subjective, music appreciation depending on taste and custom. Obtaining (tuning) the tonic (fundamental frequency) would be no problem but there are good reasons to believe that materials other than low-carbon steel can be tuned the same (significant overtones) as (except perhaps to expert tuners and musicians), or at least very similar to, the traditional steel pans, as has been demonstrated with brass in this program of research. It comes down to the skill and creativity of the tuners, who would have to get used to new materials, having had years of experience, personal and vicarious, with only one metal; e.g. steel. Because of the different material characteristics of various metals the production process (at least for hammer sinking) will vary from that of the traditional low-carbon steel, particularly for the higher range instruments (which require more deformation and have more overtones). Brass, as we have seen, requires an interstage anneal because of its higher workhardening coefficient. A similar requirement would obtain

for stainless steel, which (additionally) starts off at a considerably harder condition than low-carbon steel. Aluminum alloys would most likely have to be the age-hardenable types, to achieve the level of hardness (rigidity) for proper tuning and maintenance of the notes. Sound velocity in the material would influence the geometry of the actual note zones, brass, for example, requiring smaller sizes than steel because of its correspondingly lower sound velocity. The tuning process would also have to be altered to suit the properties of different materials (Young’s modulus for example) to achieve the required stress state and boundary conditions.

While there may be no problems in using a laboratory brass, stainless steel, or aluminum test pan, there could be problems encountered during the life of a commercial instrument in these materials. The retention time (life-time) for the tuned state of this percussion instrument is always of concern to the player. Although very preliminary, brass pan notes do not seem to remain tuned as long as carbon steel.



The formation of the pan dome by hydroforming or other methods which produce a uniform thickness may contribute to a simpler tuning routine since variations in the note thickness would be eliminated. However, it is apparent that a requisite note stability or rigidity is necessary to adequately tune and maintain the tuning and residual hardening. Nitriding and other surface metallurgical treatments have in fact been demonstrated by Schärer and Rohner [19] to be especially beneficial. From a hardness perspective it can be noted that 316L stainless steel pans formed by hammering would probably be nearly twice as hard as low-carbon steel or  $\alpha$ -brass pans (Fig. 9). However, doming would require very high temperatures for heat treatment considering the high work hardening and high melting point (Table I).

## 5. Summary and conclusions

We have demonstrated that the traditional Caribbean steel pan platform, including the standard 55-gallon barrel geometry as well as the pan metal, can be changed significantly and still maintain or improve the chromatic sounds unique to the instrument. Like many other musical instruments developed over the centuries, this flexibility will contribute to the further evolution and innovation of the only musical instrument developed in the 20th century.

Commercial cartridge brass or  $\alpha$ -brass has been used to fabricate a musical pan in the traditional style of the Caribbean steelpan but the pan platform has been expanded and no grooving was performed to isolate the note zones. Chromatic tones essentially the same as those in a low-carbon steel pan were obtained, and the results of this study demonstrate that a variety of metals or alloys could be used to fabricate a pan, including aluminum alloys.

Deformation, and correspondingly deformation microstructures, principally dislocations, have been shown to have an observable effect on the sound pulse or the amplitude-time spectrum for 316L stainless steel, low-carbon (0.06% C) steel, and 70/30,  $\alpha$ -brass, ideal, free flat, circular notes. Similar effects have also been observed for the octave ranges in the deformed/formed pan dome fabricated in the traditional way using a pneumatic hammer. However, these deformation-induced effects are not a significant feature of the note sound, but metallurgical hardness, which results from the deformation, is important in providing form and stability to the notes.

Finally, since we have demonstrated a rather radical construction of a pan by welding an  $\alpha$ -brass head to a low-carbon steel hoop and skirt with a larger diameter to create a dome with  $\sim 8\%$  more surface area, it becomes apparent that the 55-gallon barrel is not a requisite platform for pan innovations or advancements. The applications of novel joining and forming technologies combined with metallurgical processing can allow for a wide range of new musical voices and chromatic tone instrument configurations.

## Acknowledgments

This research was supported by a Mr. and Mrs. MacIntosh Murchison Endowed Chair and Dodson scholarship funds at the University of Texas at El Paso. We are grateful for the help of Jim Munson of Packaging Specialties, Inc., Medina, OH in the manufacturing of the experimental brass drums. David Brown at UTEP also provided some essential technical assistance for which we extend our gratitude. We are also grateful to the reviewer who through a very careful and insightful reading of the manuscript made very crucial and helpful comments and recommendations which were incorporated into the final manuscript.

## References

1. L. E. MURR, E. FERREYRA, J. G. MALDONADO, E. A. TRILLO, S. PAPPU, C. KENNEDY, J. DE ALBA, M. POSADA, D. P. RUSSELL and J. L. WHITE, *J. Mater. Sci.* **34** (1999) 967.
2. E. FERREYRA, J. G. MALDONADO, L. E. MURR, S. PAPPU, C. KENNEDY, M. POSADA, J. DE ALBA, R. CHITRE and D. P. RUSSELL, *ibid.* **34** (1999) 981.
3. L. E. MURR and E. FERREYRA, *Am. Sci.* **88** (2000) 38.
4. E. FERREYRA and L. E. MURR, *Mater. Characterization* **45** (2000) 341.
5. E. FERREYRA, L. E. MURR, D. P. RUSSELL and J. F. BINGERT, *ibid.* **47** (2001) 325.
6. A. ACHONG, *J. Sound & Vib.* **197** (1996) 471.
7. A. ACHONG, in Proc. Int. Conf. on the Science & Technology of the Steelpan (ICSTS 2000), edited by A. Achong (Trinidad & Tobago Govt. Printery, 2002) vol. 1, p. 1.
8. A. ACHONG, *J. Sound & Vib.* **222** (1999) 597.
9. W. SOEDEL, *ibid.* **70** (1980) 309.
10. A. ACHONG, in Proc. Int. Conf. on the Science & Technology of the Steelpan (ICSTS 2000), edited by A. Achong (Trinidad & Tobago Govt. Printery, 2002) vol. 1, p. 235.
11. T. D. ROSSING and U. J. HANSEN, "Science of the Steelpan: What is Known and What is Not," *ibid.* p. 17.
12. H. F. OLSON, "Music, Physics and Engineering," 2nd ed. (Dover, New York, 1967) p. 80.
13. L. E. MURR, "Interfacial Phenomena in Metals and Alloys" (Addison-Wesley, Reading, Mass., 1975); reprinted by Tech Books, Herndon, VA, 1991 (available form CBL, 119 Brentwood St., Marietta, OH, 45750 fax 740-374-8029).
14. DAVID R. LIDE (ed.), Handbook of Chemistry and Physics, 78th ed. (CRC Press, New York, 1997-1998).
15. D. GAY, "Steel Drums to Steelpan," in Proc. Int. Conf. on the Science and Technology of the Steelpan (ICSTS 2000), edited by A. Achong (Trinidad and Tobago Govt. Printery, 2002), vol. 1, p. 163.
16. C. A. C. IMBERT, "Investigation of Commercial Production Techniques of Steelpan Instruments," Report, Caribbean Industrial Research Institute, Tunapuna Post Office, Tunapuna, Trinidad and Tobago, 1977.
17. S. SCHÄRER, F. ROHNER and P. SCHÖBER, in Proc. Int. Conf. on the Science and Technology of the Steelpan (ICSTS 2000), edited by A. Achong (Trinidad & Tobago Govt. Printery, 2002), vol. 1, p. 189.
18. L. E. MURR, K. P. STAUDHAMMER and S. S. HECKER, *Met. Trans (A)* **13A** (1982) 627.
19. S. SCHÄRER and F. ROHNER, in Proc. Int. Conf. on the Science and Technology of the Steelpan (ICSTS 2000), edited by A. Achong (Trinidad & Tobago Govt. Printery, 2002), vol. 1, p. 179.

Received 14 August 2003  
and accepted 9 March 2004